Published in final edited form as:

Cancer Discov. 2019 May ; 9(5): 605–616. doi:10.1158/2159-8290.CD-18-0953.

Patient-driven Discovery, Therapeutic Targeting, and Post-Clinical Validation of a Novel *AKT1* Fusion-driven Cancer

Emily K Slotkin[*,1], **Daniel Diolaiti**[*,1], **Neerav N Shukla**[1], **Filemon S Dela Cruz**[1], **Jennifer J Clark**[2], **Gunes Gundem**[3], **Venkata D Yellapantula**[3], **Max F Levine**[3], **Daoqi You**[1], **Peilin Ma**[1], **Sagarika Pachhal**[1], **Glorymar Ibanez Sanchez**[1], **Ryma Benayed**[4], **Achim A Jungbluth**[4], **Lillian M Smyth**[5], **Audrey Mauguen**[3], **Irena Gushterova**[6], **Hongxu Ding**[6], **Lee Spraggon**[7], **Robert Darnell**[8], **Andrea Califano**[6], **Marc Ladanyi**[4], **Elli Papaemmanuil**[3], **Andrew L Kung**[1], **David M Hyman**[5], and **Stephen S Roberts**[1]

[1]Department of Pediatrics, Memorial Sloan Kettering Cancer Center, New York, New York

[2]Rocky Mountain Hospital for Children, Denver, Colorado

[3]Departments of Epidemiology and Biostatistics, Memorial Sloan Kettering Cancer Center, New York, New York

[4]Department of Pathology, Memorial Sloan Kettering Cancer Center, New York, New York

[5]Department of Medicine, Memorial Sloan Kettering Cancer Center, New York, New York

[6]Columbia University Medical Center, New York, New York

[7]Oxford Genetics, Oxford, United Kingdom

[8]New York Genome Center, New York, New York

Abstract

Despite the important role of the PI3K/AKT/mTOR axis in the pathogenesis of cancer, to date there have been few functional oncogenic fusions identified involving the *AKT* genes. A 12-year-old female with a histopathologically indeterminate epithelioid neoplasm was found to harbor a novel fusion between the *LAMTOR1* and *AKT1* genes. Through expanded use access, she became the first pediatric patient to be treated with the oral ATP-competitive pan-AKT inhibitor ipatasertib. Treatment resulted in dramatic tumor regression demonstrating through patient-driven discovery that the fusion resulted in activation of AKT1, was an oncogenic driver, and could be therapeutically targeted with clinical benefit. Post-clinical validation using patient-derived model systems corroborated these findings, confirmed a membrane-bound and constitutively active fusion protein, and identified potential mechanisms of resistance to single-agent treatment with ipatasertib.

Corresponding author: Emily K. Slotkin, MD, 1275 York Avenue, New York, New York 10065, Phone: 212-639-8856, Fax: 717-329-7101, slotkine@mskcc.org.

*EKS and DD contributed equally to this work

Conflict of Interest Statement: The authors certify that no actual or potential conflict of interest in relation to this article exists.

Keywords

AKT1; ipatasertib; gene fusions; pediatric cancer; mTORC1; temsirolimus

INTRODUCTION

Improved knowledge of cancer genomics has revolutionized the way we understand and treat cancer. Recurrent fusion oncoproteins are a hallmark of childhood cancer, and have been essential in investigating tumorigenesis and developing therapies (1). The *EWS-FLI1* (2) and *DNAJB1-PRKACA* (3) fusions, for example, are pathognomonic for the specific entities of Ewing sarcoma and fibrolamellar carcinoma respectively, and assist in precise diagnostics, while the *BCR-ABL* fusion has revolutionized the biologic understanding and treatment of specific leukemia subtypes (4). Despite these successes, many pathognomonic fusion oncogenes are not targetable with currently available therapies.

Despite evidence for hyperactivation or mutation of the AKT proteins and their surrounding axis in a multitude of adult-onset and subsets of pediatric malignancies (5–9), only rare oncogenic fusions, involving *AKT2* (*BCAM-AKT2*) and *AKT3* (*RPS6KC1–AKT3*) have been described and validated in ovarian cancer and breast cancer respectively (10,11). Additionally a *MAGI3-AKT3* fusion was described and initially thought to be recurrent in breast cancer (12), but thereafter could not be validated (13), and was later amended to be noted in one index case only (14). The phosphatidylinositol 3-kinase (PI3K)/AKT/mammalian target of rapamycin (mTOR) pathway regulates metabolism, homeostasis, survival, and proliferation, and is now well understood to have a role in the pathogenesis of multiple cancers (15). Despite the central role of AKT1 within this axis, there have thus far been no oncogenic fusions identified involving this gene. AKT1 is an intracellular kinase that is mutated at a low frequency across a broad range of cancers. Of more than 20,000 patient samples which have undergone targeted hybrid-based capture sequencing at our center, *AKT1 gene* is mutated in 1.7% across all samples, but in close to 6% of hormone receptor-positive breast cancers and 4% of endometrial cancers (16,17). Sixty-three percent of these mutations cause a glutamic acid to lysine substitution at amino acid 17 in the PH domain (E17K) (18,19), which was proven to be a valid therapeutic target in a recent basket trial (20).

In this report, we report the identification of *LAMTOR1-AKT1*, a novel gene fusion, and describe its patient-driven discovery, therapeutic targeting, and post-clinical validation as a tumorigenic driver and constitutive activator of AKT1.

RESULTS

Identification of a *LAMTOR1-AKT1* fusion

The patient presented at 3 years of age with abdominal swelling, pain, and elevated CA-125 levels (647 U/mL). Initial pathologic review was inconclusive despite review at multiple institutions with differential diagnoses including mesothelioma and papillary serous ovarian carcinoma. Over the following 9 years the patient had multiple surgeries, received numerous

lines of systemic therapy, targeted agents including sirolimus, pazopanib, and bevacizumab, immunotherapy with nivolumab, external beam radiation, intraperitoneal chemotherapy, and hyperthermic intraperitoneal chemotherapy (HIPEC). Targeted hybrid capture-based sequencing (21) during the patient's eighth year of treatment revealed mutations in *TP53* and the *TERT* promoter, as well as a rearrangement involving the *AKT1* gene that was reported as a variant of unknown significance.

Further examination of two tumor specimens by a second targeted hybrid capture-based sequencing assay (22) and anchored multiplex PCR (23) both confirmed the *AKT1* rearrangement and showed that it resulted in an in-frame fusion transcript joining exon 1 of Late endosomal/lysosomal Adaptor, MAPK and mTOR activator 1 (*LAMTOR1*) to exons 5–14 of *AKT1* (Fig. 1A). Structural analysis revealed that this fusion results in N-terminal truncation of AKT1, removing amino acids 1–104 which constitute 96% of the PH domain, a key regulatory domain of AKT1 (Fig. 1A). Disruption of the interaction between the PH and kinase domains has been shown to result in constitutive activation of AKT1, and mutations destabilizing this interaction can be oncogenic (24,25). Normally, the PH domain maintains AKT1 in an inactive conformation, while also mediating membrane localization in response to PI3K signaling, an essential step for AKT1 activation (26). Notably, the C-terminal LAMTOR1 residues which are part of the fusion were predicted to be myristoylated (27,28), suggesting that LAMTOR1-AKT1 may be recruited to the membrane in an inappropriately constitutive fashion. Additionally, the described fusion retains the complete kinase domain as well as the key phosphorylation sites, T308 and S473, of AKT1 (Fig. 1A), allowing for its activation. The elimination of the PH domain also suggested that the use of allosteric AKT inhibitors, known to require this region to lock AKT1 into an inactive confirmation (29,30), would have been ineffective. Based on these *in silico* predictions, the patient was treated with ipatasertib, an ATP-competitive pan-AKT inhibitor, via a compassionate use mechanism.

Anti-tumor efficacy of ipatasertib—Treatment with ipatasertib (300 mg daily) was started when the patient's CA-125 level was 10,065 U/mL in the setting of widespread disease (Fig. 1B-1). The patient tolerated the treatment well and reported a significant decrease in pain and improved energy level within one week of beginning ipatasertib. Extent of disease scans obtained at day 26 revealed markedly decreased disease burden and standardized uptake value (SUV) avidity (Fig. 1B-2). CA-125 levels were also reflective of dramatic improvement in disease burden decreasing to 7,637 and 2,637, and 1,585 U/mL on days 8, 26, and 62 days of therapy respectively (Fig. 1C). Tumor burden was additionally monitored via interrogation of plasma cell-free DNA (cfDNA) using a droplet-digital polymerase chain reaction (ddPCR) assay specific to the patient's novel fusion event (31), and was further reflective of treatment effect (Fig. 1C).

Therapy was well tolerated with the only noted adverse event being grade 1 diarrhea managed with loperamide and diphenoxylate/atropine. Grade 1 leukopenia with lowest absolute neutrophil count of 0.8 K/mcL at day 8 was noted, but resolved without growth factor support or modification of ipatasertib dosing. Rash and hyperglycemia were not noted.

After approximately 2 months of therapy the patient's CA-125 level began to rise, and by the fourth month of therapy had reached levels equivalent to those obtained prior to the initiation of ipatasertib (Fig. 1C). Repeat PET/CT imaging revealed recurrence of hypermetabolic disease (Fig. 1B-3). Targeted hybrid capture-based sequencing of a repeat biopsy obtained at this time re-identified the patient's original *AKT1* fusion, *TP53* and *TERT* mutations, as well as a new point mutation in *STAT3* (c.922A>G) which was present at a low allelic frequency of 0.07% and classified as variant of unknown significance. Notably, no secondary mutations in *AKT1* or *LAMTOR1-AKT1* were identified. Due to a lack of targetable mutations potentially responsible for resistance, we hypothesized that tumor progression was due to autocrine/paracrine activation of related pathways, and elected to add temsirolimus to her treatment regimen. Despite the addition of temsirolimus 35 mg/m^2 given on 3 occasions, the patient's disease continued to progress and the patient died of disease 5 months after initiation of ipatasertib treatment.

Pan-genomic Tumor Characterization and Classification—Additional analyses were performed simultaneously with and following the patient's treatment with ipatasertib. Whole genome (WGS) and RNA sequencing (RNA-seq) were performed on an excised lymph node with high tumor purity (estimated 75%), obtained approximately 12 weeks after ipatasertib initiation. A total of 7,407 single nucleotide variants, 641 indels, and 82 rearrangements were detected, for a total mutational burden of 2.77 mutations/Mb (Fig. 2A-D). Notable alterations included deletion of *PBRM1* (heterozygous, 10kb), *ROS1, FANCA and EML4*, and missense mutations of unknown significance in *CASC5* (c.5237C>T), *BCL11B* (c.410A>G), *STAT3* (c.922A>G), a *TP53* splice site (c.97–2AG>TT), and the *TERT* promoter (c.124C>T). Broad amplifications of chromosome 8 and arm level losses in 14q, 17p, and 18q were observed. The presence of an unbalanced translocation joining exon 1 of *LAMTOR1* and exon 5 of *AKT1* was orthogonally validated using RNA-seq analysis (Supplementary Fig. 1A). Four other fusions of unknown significance including *GNL2-EPHA10*, *STK38-MTCH1*, *PTGDS-ACTB,*and *KDM3B-GPR158-AS1* were also identified via RNA-seq (Supplementary Fig. 1B).

Clustering of the corrected variant allele frequencies (VAFs) of substitutions identified three predominant clones (Fig. 2E). Significantly, the *LAMTOR1-AKT1* fusion was present in the founder clone, and was associated with a clonal deletion event on chromosome 14 (Fig. 2E). The *TERT* promoter mutation was identified as being of potential functional significance, but was subclonal (cluster 2, 48% of cells).

Mutational signature analysis revealed that 70% of the mutations in the founder clone were assigned to signatures S-16 and S-26, which are associated with mismatch repair deficiency (32) (Supplementary Fig. 1C). The remainder of mutations in the founder clone were assigned to S-P1, a recently described signature detected in a pediatric cohort of patients associated with atypical teratoid rhabdoid tumors (33). These 3 signatures were absent in subsequent clones. This signature analysis was consistent with clonal evolution in the setting of the patient's longstanding history of high-intensity chemotherapy, in addition to endogenous mutations processes.

To further classify tumor histology, tumor gene expression was compared with samples available in The Cancer Genome Atlas (TCGA) dataset (34) and an additional cohort of neuroendocrine tumors (32 tumor types) as previously described (35,36). Results summarized on two-dimensional t-distributed stochastic neighbor embedding (t-SNE) space (Fig. 2F) and Pearson correlation coefficient heatmap (Supplementary Fig. 1D) supported mesothelioma as the closest match of this patient's tumor type, based on the close similarity to malignant pleural mesothelioma samples (TCGA), although overlap with breast and ovarian carcinomas was also noted.

Generation and validation of patient derived cells and xenograft models—To further characterize this malignancy harboring a *LAMTOR1-AKT1* fusion, patient derived cells (PDCL) and patient derived xenograft (PDX) models were established from an affected lymph node excised 26 days after the start of ipatasertib treatment (specimen code MSKCAR-65573). Both MSKCAR-65573-PDCL and MSKCAR-65573-PDX models were confirmed to harbor the fusion of interest by immunoblotting analysis (Fig. 3A-C), targeted exome sequencing (Supplementary Fig. 2A), and RT-PCR (Supplementary Fig. 2B). The LAMTOR1-AKT1 fusion appeared as a 48 kDa band recognized by antibodies developed against AKT1 C-terminal epitopes (Ab 28422, OTI 4D6), but not by antibodies recognizing the AKT1 PH domain (CST D9R8K) (Fig. 3A-C). Transient expression of LAMTOR1-AKT1 in HEK-293T cells additionally confirmed that the observed band corresponded to the LAMTOR1-AKT1 fusion protein (Supplementary Fig. 2C). Immunofluorescent and immunohistochemical analysis of MSKCAR-65573-PDCL (Fig. 3D), patient (Fig. 3E, left) and MSKCAR-65573-PDX (Fig. 3E, right) tissues showed strong positivity for membrane localized AKT1-pS473, consistent with a constitutively active, membrane-bound LAMTOR1-AKT1 fusion protein. Immunofluorescence analysis of AKT1 localization, by the use of an antibody which recognizes only the AKT1 N-terminal domain (Supplementary Fig. 2D), showed that AKT1 is predominantly, if not exclusively, localized in the cytoplasm, supporting our hypothesis that the observed membrane localized AKT1-pS473 signal was due to the LAMTOR1-AKT1 fusion protein (Supplementary Fig. 2E). Ectopic expression of an eGFP tagged LAMTOR1-AKT1 fusion protein in HeLa cells formally confirmed plasma membrane localization of LAMTOR1-AKT1 (Fig. 3F). Membrane localization was abolished by mutating the myristoylation and palmitoylation sites on the N-terminus of the LAMTOR1-AKT1 fusion protein (37), demonstrating the need for these post-translational modifications for membrane recruitment (Fig. 3F).

LAMTOR1-AKT1 is susceptible to ATP-competitive AKT inhibition

The structural domains preserved in the fusion product predicted susceptibility to ATP-competitive, but not allosteric inhibitors due to the absence of the AKT1 PH domain recognized by allosteric AKT1 inhibitors (38). To test this hypothesis, MSKCAR-65573-PDCL were incubated with either ipatasertib or allosteric AKT inhibitor MK-2206, and cell viability and activity of the AKT1/mTORC1 pathway were evaluated. As expected, ipatasertib inhibited both cell growth (Fig. 3G), as well as phosphorylation of AKT1 direct target PRAS40, and mTORC1 target RPS6 (Fig. 3H). Increased phosphorylation of AKT1 and LAMTOR1-AKT1 at both the S473 and T308 phosphorlyation sites was noted with ipatasertib treatment, as expected based on previous studies (39). While the increased

phosphorylation in AKT1 was more pronounced on S473, only LAMTOR1-AKT1 T308 phosphorylation was significantly increased by ipatasertib, while LAMTOR1-AKT1 S473 remained strongly phosphorylated and unchanged. Notably, the LAMTOR1-AKT1 fusion protein was highly phosphorylated and catalytically active in both the presence and absence of growth factor (B27 supplement), suggesting constitutive activity of the fusion protein (Fig. 3H). MK-2206 only inhibited growth at concentrations >10 μM (Fig. 3G), but did not block LAMTOR1-AKT1 signaling at any concentration tested (Fig. 3H and Supplementary Fig. 2F), indicating that the growth inhibitory effect observed at high concentrations was due to off-target effects. Ipatasertib and MK-2206 were equally effective in reducing growth of A204 cells, used as control, confirming that the lack of effect of MK-2206 in MSKCAR-65573-PDCL was specific (Supplementary Fig. 2G).

LAMTOR1-AKT1 Resistance to Ipatasertib is Mediated Through Residual mTORC1 Activity

As noted above, comparative molecular profiling of the patient's tumor when initially responsive to, and later resistant to ipatasertib therapy did not identify a genetically encoded mechanism of resistance. In *in vitro* testing, despite effective inhibition of LAMTOR1-AKT1 activity as shown by reduction of PRAS40 phosphorylation (Fig. 3H), ipatasertib did not completely inhibit tumor growth, and approximately 20% cell viability was still observed at the highest concentration tested (Fig. 3G). Additionally, residual phospho-RPS6 signal was detectable even in the presence of 1μM ipatasertib (Fig. 3H). We therefore hypothesized that residual mTORC1 activity could be responsible for the observed ipatasertib resistance, and tested various inhibitors acting on the PI3K-AKT1-mTORC1 pathway to identify the potential sources of this activity (Fig. 4A) (15,40). Among all inhibitors tested, only ipatasertib reduced PRAS40 phosphorylation (Fig. 4B). Inhibition of PI3K (using wortmannin or the more specific BKM120) or PDK1 (GSK2334470), which act upstream of LAMTOR1-AKT1, did not reduce PRAS40 phosphorylation (Fig. 4B and supplementary Fig. 3A), and only partially reduced RPS6 phosphorylation (Fig. 4B) confirming the constitutive activity of the LAMTOR1-AKT1 fusion protein. As expected, rapamycin, which directly targets the mTORC1 complex downstream of LAMTOR1-AKT1, resulted in more efficient inhibition of mTORC1 activity than ipatasertib or any other inhibitor tested, as indicated by the abolition of RPS6 phosphorylation (Fig. 4B). It has previously been shown that PDK1, through SGK1, regulates mTORC1 in an AKT-independent manner (41) conferring resistance to PI3K inhibitors, and we therefore hypothesized that a similar mechanism could be occurring in this cancer. However, inhibition of SGK1 with GSK650394 (Fig. 4B) or other specific SGK1 inhibitors (Supplementary Fig. 3B) did not reduce RPS6 phosphorylation in these cells. PDK1 inhibition with GSK2334470, however, did reduce RPS6 phosphorylation. This inhibition of mTORC1 activity as a result of inhibition of PDK1, independent of its action on LAMTOR1-AKT1 or SGK1, suggested that PDK1 acts downstream of LAMTOR1-AKT1. This is consistent with phosphorylation of p70-S6K T-229 by PDK1, a phosphorylation step that is required for the full activation of p70-S6K and subsequent RPS6 phosphorylation (42). To corroborate these findings, the status of p70-S6K-T-229 was evaluated in the presence of GSK2334470, with confirmation of reduction in phosphorylation (Supplementary Fig 3C). PDK1 phosphorylation of p70-S6K-T-229 has been reported to be independent of PI3K activity (42), in agreement with the observed lack of activity of

wortmannin on p-RPS6. Moreover, the addition of ipatasertib to PDK1 inhibitor GSK2334470 did not result in any additive effect on RPS6 phosphorylation (Supplementary Fig. 3D), confirming PDK1 inhibition acted along the same pathway and prevented RPS6 phosphorylation downstream of LAMTOR1-AKT1. Overall, these results indicated that residual mTORC1 activity, as determined by incomplete inhibition of RPS6 phosphorylation, was not due to the activation of LAMTOR1-AKT1 independent pathways, but was the result of incomplete inactivation of LAMTOR1-AKT1 activity by ipatasertib.

These concepts were further interrogated *in vivo* when mice carrying patient-derived xenograft tumors were administered either ipatasertib, the allosteric inhibitor MK-2206, or the mTORC1 inhibitor temsirolimus. Only ipatasertib and temsirolimus treatments resulted in tumor growth inhibition, while MK2206 was ineffective (Fig. 4C). Ipatasertib treatment efficiently inhibited phosphorylation of the AKT1 direct target PRAS40 and partially inhibited mTORC1 target RPS6 in the treated animals, while no changes were observed in the animals that received MK-2206 (Fig. 4D). As was similarly noted above in *in vitro* testing, temsirolimus achieved more profound inhibition of mTORC1 activity *in vivo* as shown by marked inhibition of RPS6 phosphorylation, when compared with ipatasertib treated animals (Fig. 4D). Quantification of cleaved caspase 3 and Ki67 signals after 3 days of treatment showed a statistically significant induction of apoptosis in both ipatasertib and temsirolimus treated samples, but only ipatasertib animals experienced a significant reduction in proliferation (Fig. 4E). These result show that inhibition of LAMTOR-AKT1 activity results in both decreased proliferation and increased apoptosis *in vivo*.

Despite these effects, the responses to both ipatasertib and temsirolimus were transient, and tumor regrowth was noted following approximately 3 weeks of treatment (Supplementary Fig. 3E). At day 40, phosphorylation of both PRAS40 and RPS6 in ipatasertib treated animals remained suppressed, but not abolished, confirming ongoing ipatasertib inhibitory activity (Supplementary Fig. 3F). To further identify possible mechanisms of resistance to ATP competitive AKT inhibition, we utilized a reverse phase protein array (RPPA) assay to compare ipatasertib treated animals at 3 and 40 days of treatment and directly evaluated MEK/ERK pathway activity. There was no clear upregulation of ERK activity or alternative pathways (Supplementary Fig. 3G and Supplementary Tables 1-5), confirming that tumor re-growth could have resulted from the residual mTORC1 activity observed in ipatasertib treated animals. Overall, *in vitro* and *in vivo* observations suggested that combination therapy with ATP competitive AKT inhibition as well as mTORC1 inhibition would have been necessary to provide a complete and sustained inhibition of the AKT1/mTORC1 signaling axis and tumor growth.

To formally test the hypothesis we first evaluated the effect of wortmannin, GSK2334470, and rapamycin on cell growth as single agents. GSK2334470 and rapamycin showed inhibition of cell growth as single agents, while wortmannin did not significantly reduce cell growth (Supplementary Fig. 4A). These findings are concordant with our biochemical analysis showing that wortmannin, contrary to GSK2334470 or rapamycin, did not reduce RPS6 phosphorylation. When ipatasertib administration, in combination with either GSK233470 or rapamycin was analyzed using the Chou-Talalay method (43), an additive effect was noted for both (Supplementary Figure 4B). These observations further support our

model that incomplete inactivation of the mTOR pathway downstream of LAMTOR1-AKT1 is responsible for the observed resistance.

We further proceeded to evaluate if addition of mTORC1 inhibition could overcome resistance to ipatasertib *in vivo*. MSKCAR-65573-PDX models were treated with ipatasertib or temsirolimus as single agents as well as in combination (Fig. 4F). Tumors treated with either agent alone were again noted to re-grow after approximately 3 weeks of treatment, while combination therapy inhibited tumor growth as long as animals were dosed (approximately 4 months). To confirm that tumor growth in ipatasertib treated animals was due to inefficient inhibition of mTORC1 activity, temsirolimus was administered to mice that had been treated with ipatasertib only, and an immediate inhibition of tumor growth was observed (Fig. 4G). Additionally, tumors treated with temsirolimus similarly responded to the addition of ipatasertib. These results, taken in combination with the lack of secondary mutations in *AKT1* or other candidate genes in both the patient and the MSKCAR-65573-PDX samples sequenced during periods of ipatasertib resistance (data not shown), as well as lack of upregulation of ERK or other pathways in ipatasertib resistant MSKCAR-65573-PDX tumors, corroborate residual mTORC1 activity as a mediator of resistance to ATP-competitive AKT inhibition in this *LAMTOR1-AKT1* malignancy.

DISCUSSION

This report describes a novel, activating AKT1 fusion, as well as the first use of the AKT inhibitor ipatasertib in a pediatric patient. This experience highlights the promise of real-time incorporation of molecular profiling results into clinical care, underscores the necessity of increased access to early phase agents for pediatric patients, and reveals a novel, targetable oncogenic fusion within a critical signaling pathway.

The activating LAMTOR1-AKT1 fusion described here results in the removal of nearly the entire PH domain, and is therefore hypothesized to disrupt the inhibitory interaction between the PH and kinase domain in a manner similar to that described for E17K mutations (18,24,44). Loss of the PH domain would also result in the inability of the fusion to be recruited to the plasma membrane, where AKT1 is normally activated by PDK1 and mTORC2 mediated phosphorylation. However, the presence of myristoylation and palmitoylation sites in the LAMTOR1 fusion moiety leads to LAMTOR1-AKT1 localization to the plasma membrane, thus functionally rescuing the loss of the PH domain. A similar mechanism of activation has been described for the BCAM-AKT2 fusion oncoprotein (10), strongly suggesting that membrane localization of AKT fusion proteins is a requirement for their oncogenic activity.

Stratification of adult-onset cancers has benefited from ever more rapid and cost-effective molecular profiling, but analyses of pediatric cancers have not yielded similar successes for children and young adults. This disparity has been traditionally attributed to the relatively undisturbed pediatric cancer genome in the setting of a paucity of applicable and available compounds. This experience adds to several prominent examples including the use of assembly-based whole-genome DNA sequencing to discover previously undefined rearrangements in rhabdoid tumors (45), and the finding of genomic rearrangements in

telomerase reverse transcriptase gene (*TERT*) (46) in high-risk neuroblastoma, which highlight the need for broad and comprehensive approaches to molecular profiling, particularly in pediatric cancers. Analysis of whole genome sequencing revealed that the overall mutational burden (2.77 subs/Mb) in this patient's tumor was higher than typical for a majority of pediatric cancers (32,47), most likely due to significant pre-treatment with known genotoxic agents including platinum compounds. In spite of this relatively high mutational burden, there was a rapid and dramatic clinical response to ipatasertib treatment, supporting this novel fusion as the primary oncogenic driver in this cancer.

It is most notable that the use of ipatasertib in this patient was driven by rapid, *in silico* analyses with the ensuing hypothesis that the identified *LAMTOR1-AKT1* fusion could be an oncogenic driver. The compassionate use of ipatasertib in this setting had not been validated in either the pre-clinical or clinical setting and, furthermore, had not been administered to a pediatric patient. Instead, it was this patient's experience itself, followed by what can be referred to as "post-clinical validation," that now corroborates these initial hypotheses. Under such circumstances it would not have been practical or beneficial to the patient to proceed in the traditional, and reverse, fashion, allowing time for pre-clinical confirmation before administering the drug. With the deluge of ever more quickly available molecular profiling, we suspect such opportunities will become routine, and a paradigm to proceed from sequencing or other similar personalized data to individualized clinical trial, followed by or simultaneous with post-clinical validation will be accepted even in pediatric patients.

The coming together of multiple clinical, research, and regulatory platforms and sources of expertise facilitated the discovery, therapeutic targeting, and characterization of the first described oncogenic *AKT1* gene fusion. The first-ever pediatric use of a well-tolerated, orally bioavailable, ATP-competitive AKT kinase inhibitor, ipatasertib, validated this molecular event as an oncogenic driver, and was successful in inducing a dramatic clinical response. However, as is common with single-agent targeted inhibition, resistance was noted and precluded durable response. Our experience is complementary to the results of an ipatasertib phase I clinical trial in adult-onset cancers, in which the most responsive patients carried alterations in the PI3K pathway, but achieved only stable disease at best (20). Our post-clinical analyses provide insights into possible mechanisms of resistance to single-agent ipatasertib therapy, suggesting that in these *LAMTOR1-AKT1* fusion driven models, ipatasertib treatment as a single agent was not sufficient to completely inhibit mTORC1 activity, and that this residual activity precluded more durable response. These observations suggest that combination ATP-competitive AKT and mTORC1 inhibition is rational, may be successful in overcoming resistance to single-agent AKT inhibition, and can be considered for future clinical trials focused on malignancies with analogous AKT activating mutations. We note that while we administered the combination of ipatasertib and temsirolimus in the described patient following progression on ipatasertib alone, these agents were given in combination very briefly during a period of profound illness secondary to multi-organ failure in the setting of widespread disease progression, and her experience during this period must therefore be interpreted with caution. Additionally, the patient did receive sirolimus (in combination with bevacizumab and irinotecan, and later in combination with pazopanib) prior to her exposure to ipatasertib, on which some transient stability of disease

was noted on both regimens, followed by progression of disease. Further work is warranted to achieve a more comprehensive understanding of the biologic implications of the described fusion and the prevalence and role of this or other *AKT1* fusions in human cancers.

MATERIALS AND METHODS

Clinical Care

Written informed consent and verbal assent was obtained from the patient's guardian and the patient respectively for treatment with ipatasertib. All studies were conducted in accordance with recognized ethical guidelines including the Belmont Report and the U.S. Common Rule, and all studies were approved by an institutional review board.

Reagents

pBABE–puro retroviral vector was purchased from Addgene. Ipatasertib, MK-2206, temsirolimus, SGK233470, wortmannin, rapamycin, and SGK650394 were purchased from Selleckchem. SGK1 inhibitors compound 14g and mp-1 were provided by Dr. Marc Nazare (Leibniz-Forschungsinstitut für Molekulare Pharmakologie (FMP)). Unless specified, all *in vitro* treatments were performed using 1μM concentration for 3 hours.

Animal studies

The patient derived xenograft (PDX) model (code: MSKCAR-65573, specimen 0002a) was developed by transplanting a tumor sample from the patient's lymph node into the flank of NOD (NOD.Cg-Prkdc^{scid} Il2rg^{tm1Wjl}/SzJ) scid gamma (NSG) mice to generate the passage 0 (P0) generation. Upon reaching a tumor width of ~1 cm, the PDX P0 tumors were collected and expanded into a larger cohort. Animals were dosed with single agents ipatasertib 100mg/kg/day (oral gavage), or temsirolimus 20mg/kg/day (intraperitoneal injection), or MK-2206 100mg/kg/day (oral gavage). When combination treatment was administered doses were reduced to ipatasertib 75 mg/kg/day and temsirolimus 10 mg/kg three days per week to avoid excessive toxicity. All experiments were performed in accordance with institutional guidelines and under an approved protocol from The Memorial Sloan Kettering Cancer Center Institutional Animal Care and Use Committee (protocol number 16–08-011).

Cell lines and primary cells

HEK-293T and HeLa cells were obtained from American Type Culture Collection (ATCC) and were maintained in DMEM, 10% FBS, penicillin/streptomycin and fungizone with a doubling time of ~ 72 hours. MSKCAR-65573-CL cells were generated from the MSKCAR-65573-PDX p0 model by harvesting tumors, mincing into 2–4 mm pieces, and dissociating using the Tumor Dissociation Kit (MACS, Miltenyi Biotec) on a MACS Octo Dissociator with Heaters (Miltenyi Biotec) at 37°C for 60 minutes under continuous rotation. The cell line MSKCAR-65573-CL was established in neurobasal media + B27 supplement. All cells were tested for mycoplasma as previously described (48) approximately once every 4 months (last performed October, 2018).

Transient expression

The coding sequences of AKT1, LAMTOR1-AKT1 fusion construct, and mutant LAMTOR1-AKT1 (G2A) or (C3S, C4S) were synthesized by Genscript (Piscataway, NJ) in vector pUC57. Coding sequences were cloned into the pcDNA3.1-C-eGFP expression vector between the BamHI and KpnI restriction sites in frame with N-terminal eGFP. Transfection of 293T or Hela cells was performed using Lipofectamine 3000 (Invitrogen) according to the manufacturer's guidelines.

Cell viability assay

Cells (2,500 cells/well) were seeded in 96-well plates and after 24 hours were incubated with either single drugs (ipatsertib, MK-2206, GSK1904529A, wortmannin, GSK2334470, rapamycin, KU-0063794, or GSK650394) for 72 hours. The viability of the cells was determined using Celltiter-Glo Luminescent Cell Viability Assay (Promega). IC_{50} concentrations were determined using GraphPad Prism Software.

Genomic characterization

Targeted hybridization capture DNA sequencing, anchored multiplex RNA sequencing, whole-genome sequencing, RNA sequencing and t-SNE are described in detail in supplementary materials and methods.

Plasma cell-free DNA extraction, analysis, and patient specific droplet digital polymerase chain reaction

These investigations were carried out as has been previously described (31).

Supplementary Material

Refer to Web version on PubMed Central for supplementary material.

Acknowledgements

The authors would like to thank ArcherDX, Inc. and Array BioPharma for assistance in characterizing the novel *LAMTOR1-AKT1* fusion, Roche/Genentech for supplying ipatasertib, Dr. Elisa de Stanchina and the MSKCC Antitumor Assessment Core Facility for assistance in performing *in vivo* testing, Dr. Marc Nazare for providing SGK1 inhibitors mp-1 and cmp-14, Jessie Hillsberg for her caring treatment of the patient, and Drs. Todd Heaton and Michael P. LaQuaglia for their support in obtaining biopsies.

Financial support: Funding for this work was generously provided by the Sohn Conference Foundation, The PaulieStrong Foundation, Cycle for Survival (Team Kate in memory of Kate Hennemuth Reap), the Olayan Precision Pediatrics Program, and the NCI grant P30 CA008748.

References

1. Mitelman F, Johansson B, Mertens F. The impact of translocations and gene fusions on cancer causation. Nat Rev Cancer 2007;7(4):233–45 doi 10.1038/nrc2091. [PubMed: 17361217]
2. Delattre O, Zucman J, Plougastel B, Desmaze C, Melot T, Peter M, et al. Gene fusion with an ETS DNA-binding domain caused by chromosome translocation in human tumours. Nature 1992;359(6391):162–5 doi 10.1038/359162a0. [PubMed: 1522903]
3. Honeyman JN, Simon EP, Robine N, Chiaroni-Clarke R, Darcy DG, Lim II, et al. Detection of a recurrent DNAJB1-PRKACA chimeric transcript in fibrolamellar hepatocellular carcinoma. Science 2014;343(6174):1010–4 doi 10.1126/science.1249484. [PubMed: 24578576]

4. Ren R Mechanisms of BCR-ABL in the pathogenesis of chronic myelogenous leukaemia. Nat Rev Cancer 2005;5(3):172–83 doi 10.1038/nrc1567. [PubMed: 15719031]

5. Opel D, Poremba C, Simon T, Debatin KM, Fulda S. Activation of Akt predicts poor outcome in neuroblastoma. Cancer Res 2007;67(2):735–45 doi 10.1158/0008-5472.CAN-06-2201. [PubMed: 17234785]

6. Toretsky JA, Thakar M, Eskenazi AE, Frantz CN. Phosphoinositide 3-hydroxide kinase blockade enhances apoptosis in the Ewing's sarcoma family of tumors. Cancer Res 1999;59(22):5745–50. [PubMed: 10582694]

7. Cen L, Arnoczky KJ, Hsieh FC, Lin HJ, Qualman SJ, Yu S, et al. Phosphorylation profiles of protein kinases in alveolar and embryonal rhabdomyosarcoma. Mod Pathol 2007;20(9):936–46 doi 10.1038/modpathol.3800834. [PubMed: 17585318]

8. Perry JA, Kiezun A, Tonzi P, Van Allen EM, Carter SL, Baca SC, et al. Complementary genomic approaches highlight the PI3K/mTOR pathway as a common vulnerability in osteosarcoma. Proc Natl Acad Sci U S A 2014;111(51):E5564–73 doi 10.1073/pnas.1419260111. [PubMed: 25512523]

9. Wu G, Diaz AK, Paugh BS, Rankin SL, Ju B, Li Y, et al. The genomic landscape of diffuse intrinsic pontine glioma and pediatric non-brainstem high-grade glioma. Nat Genet 2014;46(5):444–50 doi 10.1038/ng.2938. [PubMed: 24705251]

10. Kannan K, Coarfa C, Chao PW, Luo L, Wang Y, Brinegar AE, et al. Recurrent BCAM-AKT2 fusion gene leads to a constitutively activated AKT2 fusion kinase in high-grade serous ovarian carcinoma. Proceedings of the National Academy of Sciences of the United States of America 2015;112(11):E1272–7 doi 10.1073/pnas.1501735112. [PubMed: 25733895]

11. Matissek KJ, Onozato ML, Sun S, Zheng Z, Schultz A, Lee J, et al. Expressed Gene Fusions as Frequent Drivers of Poor Outcomes in Hormone Receptor-Positive Breast Cancer. Cancer discovery 2018;8(3):336–53 doi 10.1158/2159-8290.CD-17-0535. [PubMed: 29242214]

12. Banerji S, Cibulskis K, Rangel-Escareno C, Brown KK, Carter SL, Frederick AM, et al. Sequence analysis of mutations and translocations across breast cancer subtypes. Nature 2012;486(7403): 405–9 doi 10.1038/nature11154. [PubMed: 22722202]

13. Mosquera JM, Varma S, Pauli C, MacDonald TY, Yashinskie JJ, Varga Z, et al. MAGI3-AKT3 fusion in breast cancer amended. Nature 2015;520(7547):E11–2 doi 10.1038/nature14265. [PubMed: 25877206]

14. Pugh TJ, Banerji S, Pugh Meyerson M. et al. reply. Nature 2015;520(7547):E12–4 doi 10.1038/nature14266. [PubMed: 25877207]

15. Vivanco I, Sawyers CL. The phosphatidylinositol 3-Kinase AKT pathway in human cancer. Nat Rev Cancer 2002;2(7):489–501 doi 10.1038/nrc839. [PubMed: 12094235]

16. Cerami E, Gao J, Dogrusoz U, Gross BE, Sumer SO, Aksoy BA, et al. The cBio cancer genomics portal: an open platform for exploring multidimensional cancer genomics data. Cancer Discov 2012;2(5):401–4 doi 10.1158/2159-8290.CD-12-0095. [PubMed: 22588877]

17. Zehir A, Benayed R, Shah RH, Syed A, Middha S, Kim HR, et al. Mutational landscape of metastatic cancer revealed from prospective clinical sequencing of 10,000 patients. Nat Med 2017;23(6):703–13 doi 10.1038/nm.4333. [PubMed: 28481359]

18. Carpten JD, Faber AL, Horn C, Donoho GP, Briggs SL, Robbins CM, et al. A transforming mutation in the pleckstrin homology domain of AKT1 in cancer. Nature 2007;448(7152):439–44 doi 10.1038/nature05933. [PubMed: 17611497]

19. Chang MT, Asthana S, Gao SP, Lee BH, Chapman JS, Kandoth C, et al. Identifying recurrent mutations in cancer reveals widespread lineage diversity and mutational specificity. Nat Biotechnol 2016;34(2):155–63 doi 10.1038/nbt.3391. [PubMed: 26619011]

20. Hyman DM, Smyth LM, Donoghue MTA, Westin SN, Bedard PL, Dean EJ, et al. AKT Inhibition in Solid Tumors With AKT1 Mutations. J Clin Oncol 2017;35(20):2251–9 doi 10.1200/JCO.2017.73.0143. [PubMed: 28489509]

21. Frampton GM, Fichtenholtz A, Otto GA, Wang K, Downing SR, He J, et al. Development and validation of a clinical cancer genomic profiling test based on massively parallel DNA sequencing. Nat Biotechnol 2013;31(11):1023–31 doi 10.1038/nbt.2696. [PubMed: 24142049]

22. Cheng DT, Mitchell TN, Zehir A, Shah RH, Benayed R, Syed A, et al. Memorial Sloan Kettering-Integrated Mutation Profiling of Actionable Cancer Targets (MSK-IMPACT): A Hybridization

Capture-Based Next-Generation Sequencing Clinical Assay for Solid Tumor Molecular Oncology. J Mol Diagn 2015;17(3):251–64 doi 10.1016/j.jmoldx.2014.12.006. [PubMed: 25801821]

23. Zheng Z, Liebers M, Zhelyazkova B, Cao Y, Panditi D, Lynch KD, et al. Anchored multiplex PCR for targeted next-generation sequencing. Nat Med 2014;20(12):1479–84 doi 10.1038/nm.3729. [PubMed: 25384085]
24. Parikh C, Janakiraman V, Wu WI, Foo CK, Kljavin NM, Chaudhuri S, et al. Disruption of PH-kinase domain interactions leads to oncogenic activation of AKT in human cancers. Proc Natl Acad Sci U S A 2012;109(47):19368–73 doi 10.1073/pnas.1204384109. [PubMed: 23134728]
25. Kumar A, Purohit R. Cancer Associated E17K Mutation Causes Rapid Conformational Drift in AKT1 Pleckstrin Homology (PH) Domain. Plos One 2013;8(5) doi ARTN e64364 10.1371/journal.pone.0064364.
26. Andjelkovic M, Alessi DR, Meier R, Fernandez A, Lamb NJ, Frech M, et al. Role of translocation in the activation and function of protein kinase B. J Biol Chem 1997;272(50):31515–24. [PubMed: 9395488]
27. Maurer-Stroh S, Eisenhaber B, Eisenhaber F. N-terminal N-myristoylation of proteins: prediction of substrate proteins from amino acid sequence. J Mol Biol 2002;317(4):541–57 doi 10.1006/jmbi.2002.5426. [PubMed: 11955008]
28. Maurer-Stroh S, Eisenhaber B, Eisenhaber F. N-terminal N-myristoylation of proteins: refinement of the sequence motif and its taxon-specific differences. J Mol Biol 2002;317(4):523–40 doi 10.1006/jmbi.2002.5425. [PubMed: 11955007]
29. Barnett SF, Defeo-Jones D, Fu S, Hancock PJ, Haskell KM, Jones RE, et al. Identification and characterization of pleckstrin-homology-domain-dependent and isoenzyme-specific Akt inhibitors. Biochem J 2005;385(Pt 2):399–408 doi 10.1042/BJ20041140. [PubMed: 15456405]
30. Kumar CC, Madison V. AKT crystal structure and AKT-specific inhibitors. Oncogene 2005;24(50):7493–501 doi 10.1038/sj.onc.1209087. [PubMed: 16288296]
31. Shukla NN, Patel JA, Magnan H, Zehir A, You D, Tang J, et al. Plasma DNA-Based Molecular Diagnosis, Prognostication, and Monitoring of Patients With EWSR1 Fusion-Positive Sarcomas. JCO Precision Oncology 2017(1):1–11 doi 10.1200/po.16.00028.
32. Alexandrov LB, Nik-Zainal S, Wedge DC, Aparicio SA, Behjati S, Biankin AV, et al. Signatures of mutational processes in human cancer. Nature 2013;500(7463):415–21 doi 10.1038/nature12477. [PubMed: 23945592]
33. Grobner SN, Worst BC, Weischenfeldt J, Buchhalter I, Kleinheinz K, Rudneva VA, et al. The landscape of genomic alterations across childhood cancers. Nature 2018;555(7696):321–7 doi 10.1038/nature25480. [PubMed: 29489754]
34. Cancer Genome Atlas Research N, Weinstein JN, Collisson EA, Mills GB, Shaw KR, Ozenberger BA, et al. The Cancer Genome Atlas Pan-Cancer analysis project. Nat Genet 2013;45(10):1113–20 doi 10.1038/ng.2764. [PubMed: 24071849]
35. Dela Cruz FS, Diolaiti D, Turk AT, Rainey AR, Ambesi-Impiombato A, Andrews SJ, et al. A case study of an integrative genomic and experimental therapeutic approach for rare tumors: identification of vulnerabilities in a pediatric poorly differentiated carcinoma. Genome Med 2016;8(1):116 doi 10.1186/s13073-016-0366-0. [PubMed: 27799065]
36. Maaten LHG. Visualizing data using t-SNE. Journal of Machine Learning Research 2008;9(Nov): 2579–605.
37. Nada S, Mori S, Takahashi Y, Okada M. p18/LAMTOR1: a late endosome/lysosome-specific anchor protein for the mTORC1/MAPK signaling pathway. Methods Enzymol 2014;535:249–63 doi 10.1016/B978-0-12-397925-4.00015-8. [PubMed: 24377928]
38. Rehan M, Beg MA, Parveen S, Damanhouri GA, Zaher GF. Computational insights into the inhibitory mechanism of human AKT1 by an orally active inhibitor, MK-2206. PLoS One 2014;9(10):e109705 doi 10.1371/journal.pone.0109705. [PubMed: 25329478]
39. Okuzumi T, Fiedler D, Zhang C, Gray DC, Aizenstein B, Hoffman R, et al. Inhibitor hijacking of Akt activation. Nat Chem Biol 2009;5(7):484–93 doi 10.1038/nchembio.183. [PubMed: 19465931]

40. Dienstmann R, Rodon J, Serra V, Tabernero J. Picking the point of inhibition: a comparative review of PI3K/AKT/mTOR pathway inhibitors. Molecular cancer therapeutics 2014;13(5):1021–31 doi 10.1158/1535-7163.MCT-13-0639. [PubMed: 24748656]

41. Castel P, Ellis H, Bago R, Toska E, Razavi P, Carmona FJ, et al. PDK1-SGK1 Signaling Sustains AKT-Independent mTORC1 Activation and Confers Resistance to PI3Kalpha Inhibition. Cancer Cell 2016;30(2):229–42 doi 10.1016/j.ccell.2016.06.004. [PubMed: 27451907]

42. Pullen N, Dennis PB, Andjelkovic M, Dufner A, Kozma SC, Hemmings BA, et al. Phosphorylation and activation of p70s6k by PDK1. Science 1998;279(5351):707–10. [PubMed: 9445476]

43. Chou TC. Drug combination studies and their synergy quantification using the Chou-Talalay method. Cancer Res 2010;70(2):440–6 doi 10.1158/0008-5472.CAN-09-1947. [PubMed: 20068163]

44. Jo H, Lo PK, Li Y, Loison F, Green S, Wang J, et al. Deactivation of Akt by a small molecule inhibitor targeting pleckstrin homology domain and facilitating Akt ubiquitination. Proc Natl Acad Sci U S A 2011;108(16):6486–91 doi 10.1073/pnas.1019062108. [PubMed: 21464312]

45. Henssen AG, Koche R, Zhuang J, Jiang E, Reed C, Eisenberg A, et al. PGBD5 promotes site-specific oncogenic mutations in human tumors. Nature genetics 2017;49(7):1005–14 doi 10.1038/ng.3866. [PubMed: 28504702]

46. Peifer M, Hertwig F, Roels F, Dreidax D, Gartlgruber M, Menon R, et al. Telomerase activation by genomic rearrangements in high-risk neuroblastoma. Nature 2015;526(7575):700–4 doi 10.1038/nature14980. [PubMed: 26466568]

47. Downing JR, Wilson RK, Zhang J, Mardis ER, Pui CH, Ding L, et al. The Pediatric Cancer Genome Project. Nature genetics 2012;44(6):619–22 doi 10.1038/ng.2287. [PubMed: 22641210]

48. Mariotti E, Mirabelli P, Di Noto R, Fortunato G, Salvatore F. Rapid detection of mycoplasma in continuous cell lines using a selective biochemical test. Leuk Res 2008;32(2):323–6 doi 10.1016/j.leukres.2007.04.010. [PubMed: 17586045]

SIGNIFICANCE

This study describes the patient-driven discovery of the first AKT1 fusion driven cancer and its treatment with the AKT inhibitor, ipatasertib. Patient derived *in vitro* and *in vivo* model systems are used to confirm the LAMTOR1-AKT1 fusion as a tumorigenic driver, and identify potential mechanisms of resistance to AKT inhibition.

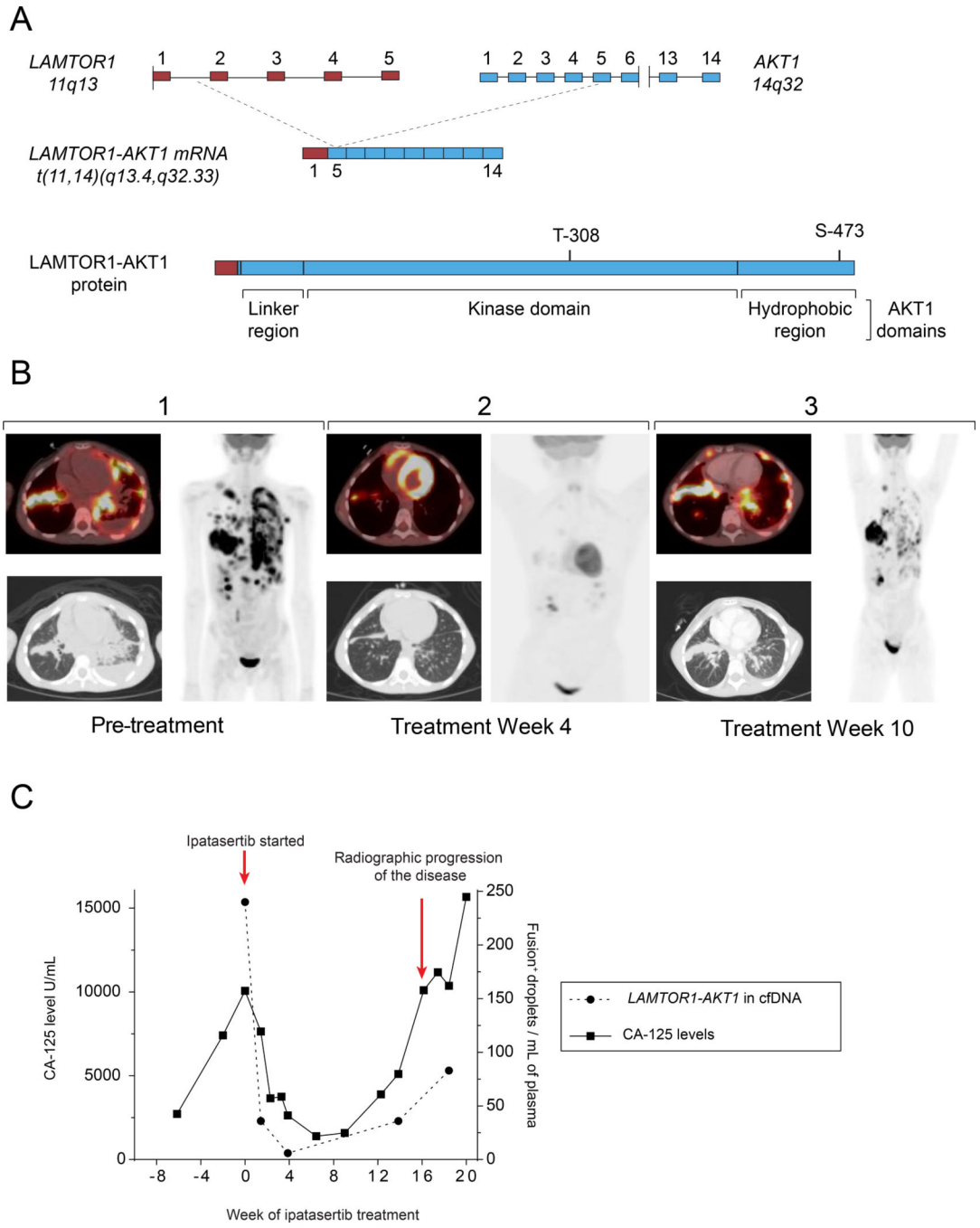

Figure 1. A Novel *AKT1* Fusion-Driven Cancer.

A) Schematic diagram of the genomic DNA, mRNA, and protein structures of the *LAMTOR1-AKT1 t(11,14)(q.13.4, q32.33)* fusion; the top panel illustrates the fusion breakpoints within intron 1 of *LAMTOR1* (red) and exon 5 of *AKT1* (blue); the middle panel illustrates the resulting fusion mRNA structure; the bottom panel illustrates the protein structure, including the near-total removal of AKT1 PH domain, the retention of the entire kinase domain, and both phosphorylation sites (T308, S473). **B)** Representative computed tomography (CT) images of the chest and whole-body projections from

^{18}fluorodeoxyglucose (FDG)-PET scans are shown; Panel 1 depicts tumor burden at the start of treatment with AKT inhibitor ipatasertib; Panel 2 depicts repeat imaging following 4 weeks of treatment with ipatasertib; Panel 3 depicts repeat imaging following 10 weeks of therapy. **C)** Dual axis graph comparing levels of the patient's established tumor marker, CA-125, and the number of *LAMTOR1*-AKT1 fusion positive droplets per mL of plasma via a cell-free DNA assay over time

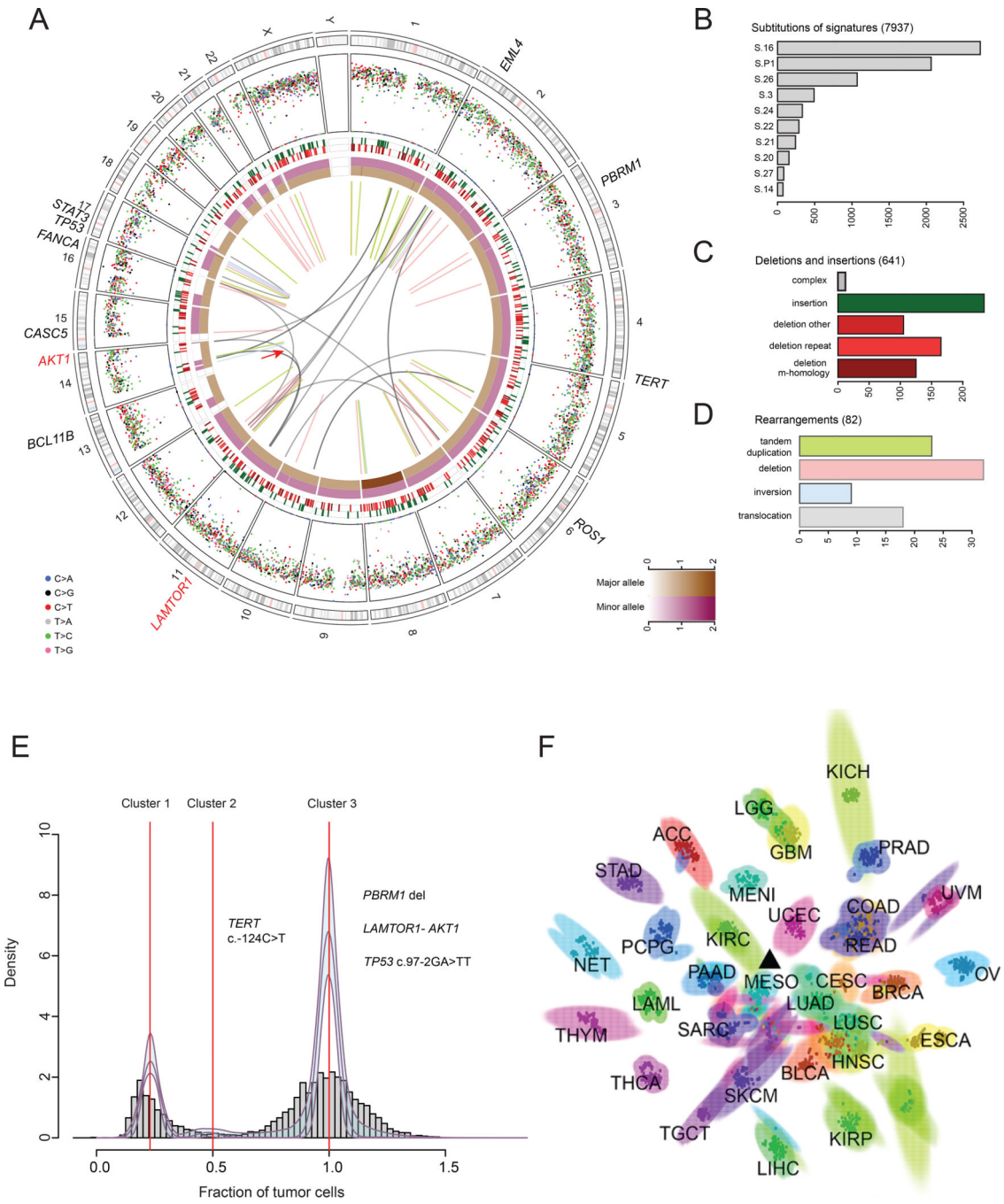

Figure 2. Pan-Genomic Analysis of a Novel AKT1 Fusion-Driven Pediatric Cancer.

A) Circos plot summarizing whole genome sequencing analysis with the novel *LAMTOR1-AKT1* fusion marked by a red arrow; the two innermost tracks depict the integer copy number changes for the major (brown) and minor allele (dark pink); the outermost track shows the inter-mutation distance for substitutions each plotted according to the type of nucleotide change; the middle track shows the genomic positions of the small insertion (green) and deletion (red) along the genome; rearrangements are plotted as arcs inside the circos; labeled genes show aberrations in genes present in Cancer Genes Census **B)**

Mutation signature analysis using deconstructSigs. **C)** Summary of the insertion and deletion data **D)** Summary of rearrangement data **E)** Distribution of corrected variant allele frequency (VAF) identifying the *LAMTOR1-AKT1* fusion as a founder clonal event **F)** Scatter-plot showing the t-SNE 2D projection of 2400 samples, including at least 75 samples (indicated in the figure) for each of the 32 tissue types represented; the described patient's tissue is indicated by a black triangle; tumor type abbreviations: ACC adrenocortical carcinoma, BLCA bladder urothelial carcinoma, BRCA breast carcinoma, CESC cervical carcinoma, COAD colon adenocarcinoma, ESCA esophageal carcinoma, GBM glioblastoma multiforme, HNSC head and neck carcinoma, KICH kidney chromophobe, KIRC clear cell carcinoma of the kidney, KIRP renal papillary cell carcinoma, LAML acute myeloid leukemia, LGG low grade glioma, LIHC hepatocellular carcinoma, LUAD lung adenocarcinoma, LUSC lung squamous cell carcinoma, MENI meningioma, MESO mesothelioma, NET gastrointestinal neuroendocrine tumor, OV ovarian carcinoma, PAAD pancreatic adenocarcinoma, PCPG pheochromocytoma and paraganglioma, PRAD prostate adenocarcinoma, READ rectal adenocarcinoma, SARC sarcoma, SKCM cutaneous melanoma, STAD gastric adenocarcinoma, TGCT testicular germ cell tumor, THCA thyroid carcinoma, THYM thymoma, UCEC uterine corpus endometrial carcinoma, UVM uveal melanoma

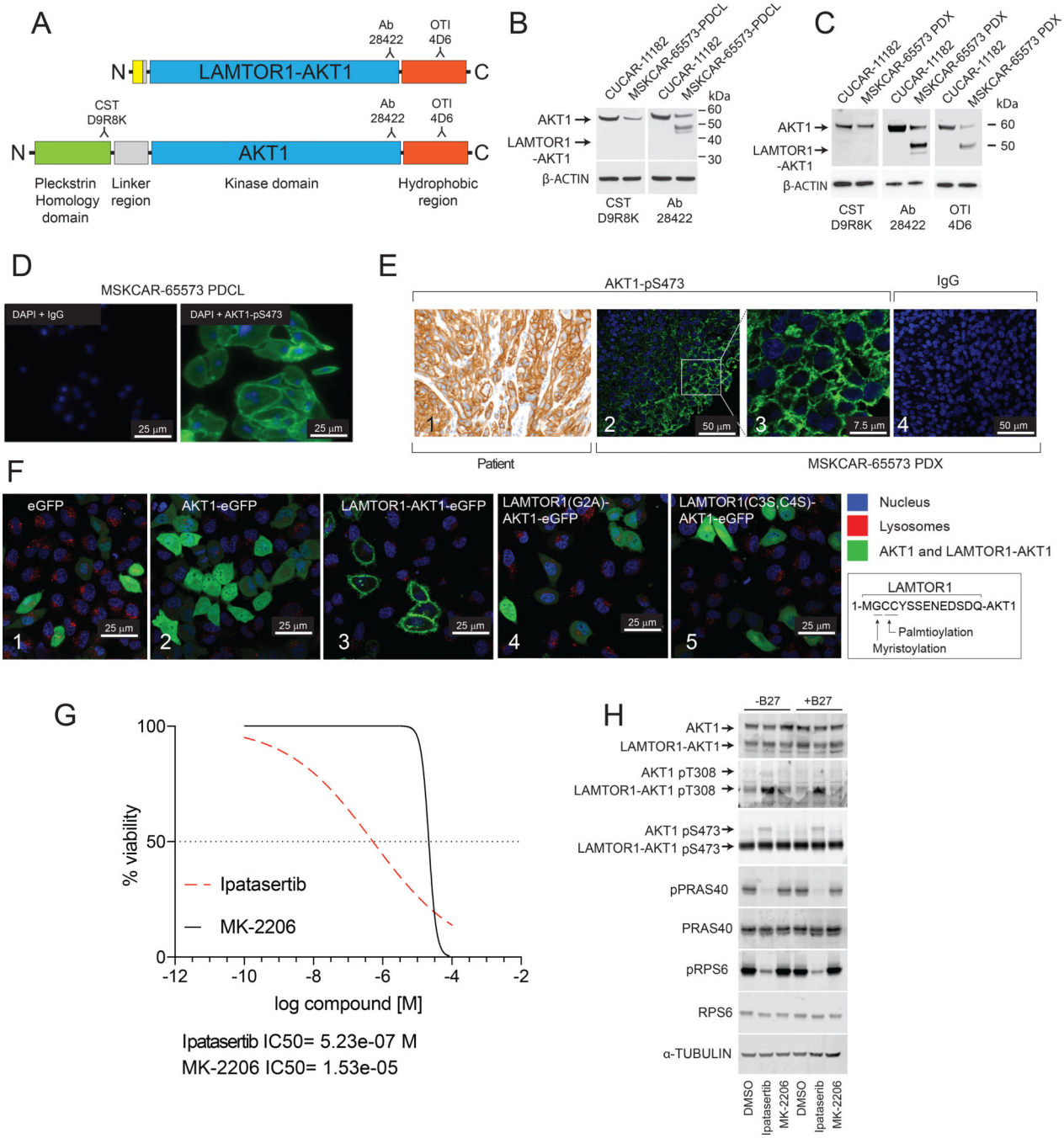

Figure 3. Generation and Validation of Patient Derived Cell Line and Xenograft Models and Confirmation of LAMTOR1-AKT1 Membrane Localization.

A) Schematic localization of the epitopes recognized by the indicated anti-AKT1 antibodies (CST-D9R8K, Ab-28422 and OTI-4D6) which were used to confirm the presence of the LAMTOR1-AKT1 fusion in patient-derived cell line (PDCL) and patient derived xenograft (PDX) models **B)** Immunoblotting analysis confirming the expression of the LAMTOR1-AKT1 fusion protein in the PDCL (MSKCAR-65573-PDCL); cells derived from a previously described undifferentiated carcinoma (CUCAR-11182) expressing AKT1 were

used as control **C)** Immunoblotting analysis confirming the expression of the LAMTOR1-AKT1 fusion protein in the PDX tissue (MSKCAR-65573) **D)** Immunofluorescence of AKT1-pS473 in PDCL **E)** Panel 1 depicts a high-powered view of immunohistochemical analysis of AKT1-pS473 (brown) in the patient's sample confirming marked membrane localization; Panels 2 and 3 depict low and high-powered views, respectively, of immunofluorescent analysis of AKT1-pS473 (green) and its plasma membrane localization in the PDX (MSKCAR-65573-PDCL) model; Panel 4 depicts IgG control **F)** Panels 1–5 depict representative images of HeLa cells transfected with plasmids encoding the indicated proteins fused to eGFP (N-terminus) (Blue: Hoechst 33342; Red: LysoTraker DND-99; Green: GFP or eGFP labeled protein); LysoTraker DND-99 red staining was included as control to evaluate lysosomal localization; the sequence depicted in the box represents the first 14 amino acids of the LAMTOR1-AKT1 fusion including the myristoylation and palmitoylation sites; panels 4 and 5 depict the lack of membrane localization following mutation of the noted myristoylation and palmitoylation sites **G)** Evaluation of the anti-proliferative effect of ipatasertib and MK-2206 on the PDX model (MSKCAR-65573-PDCL) *in vitro* **H)** Immunoblotting analysis of the indicated proteins in the PDX model (MSKCAR-65573-PDCL) upon treatment with ipatasertib or MK-2206 in the presence and absence of serum growth factor B27

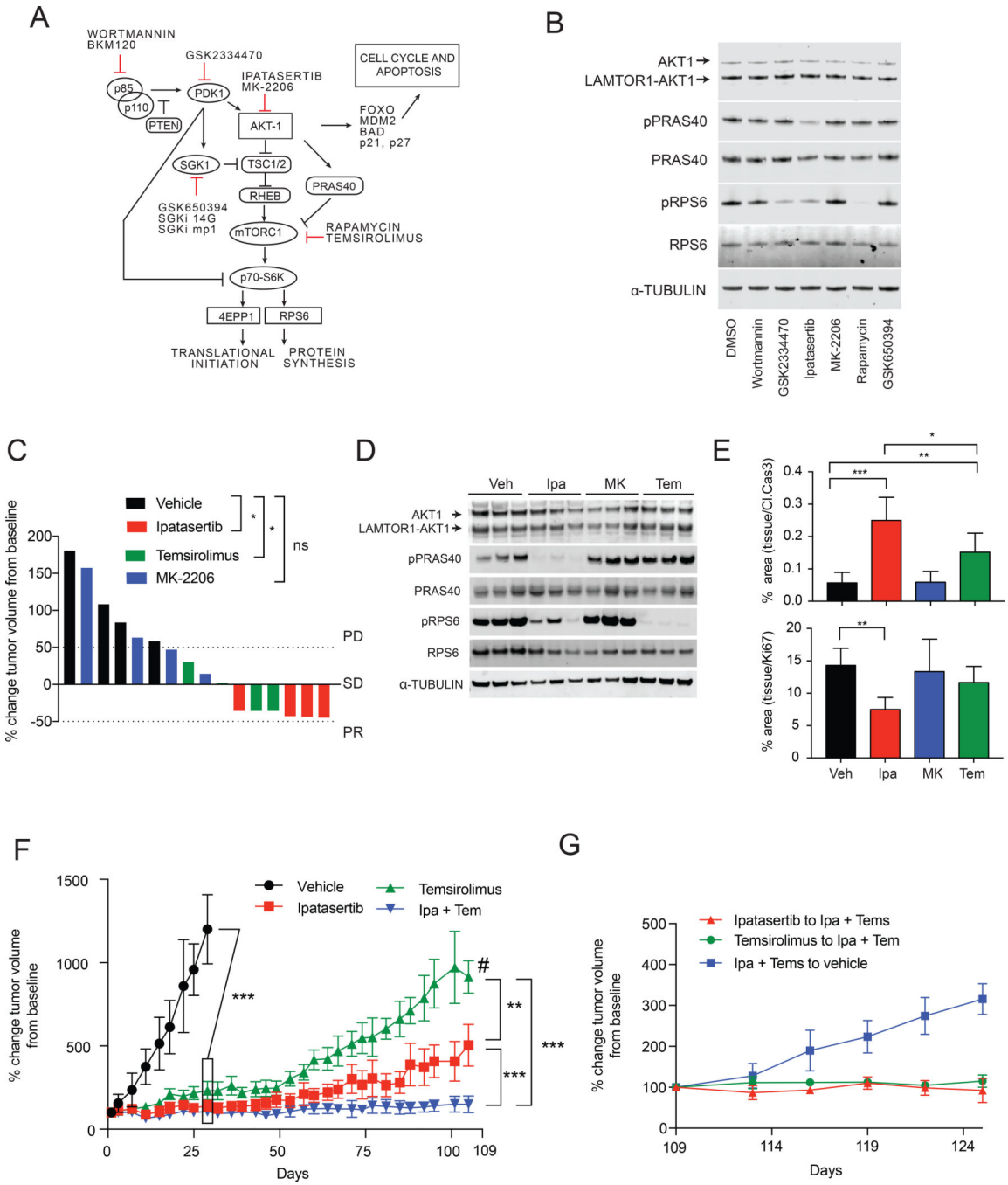

Figure 4. Dual Inhibition of LAMTOR1-AKT1 and mTORC1 is Necessary to Inhibit Tumor Growth.

A) Schematic representation of the PI3K-AKT-mTORC1 axis and the target of each inhibitor **B)** Immunoblotting analysis of selected proteins in presence of the indicated inhibitors **C)** Waterfall plot showing patient derived xenograft (PDX) (MSKCAR-65573) tumor size changes after 15 days of treatment (best response) with either ipatasertib, MK-2206 or temsirolimus; response was classified as progressive disease (>50% tumor volume increase), stable disease (between 50% increase and 50% reduction) or partial

response (>50% tumor volume reduction) and each column represents a single animal **D)** Immunoblotting analysis of indicated proteins in tumors after 3 days of treatment with ipatasertib (Ipa), MK2206 (MK), temsirolimus (Tem) or vehicle (Veh) **E)** Immunohistochemical quantification of apoptosis (cleaved caspase 3 signal, Cl.Cas3) and proliferation (Ki67 signal) in tumor tissues treated for three days with the indicated drugs; mean and standard deviation of tumor tissue obtained from three independent mice per group are shown and one-way ANOVA analysis is used; *=$p<0.05$, **=$p<0.01$, ***=$p<0.001$ **F)** Growth curve plot of tumor response to continuous vehicle, ipatasertib, temsirolimus, or ipatasertib + temsirolimus treatments; # indicates a decrease in tumor volume at day 109 due to the censoring of two mice having ulcerated tumors **G)** Growth curve plot of tumor volume changes after interruption of treatment in the combination arm or addition of ipatasertib or temsirolimus to the reciprocal single agent treatments; tumor volumes were normalized to tumor volumes recorded at the time treatment was modified (day 109); *=$p<0.05$, **=$p<0.01$, ***=$p<0.001$; the Fisher exact test was used to evaluate the statistical significance of the difference between groups in panel E; area under the curve (AUC) analysis was used for panel F